MITIGATION OF SCC AND CORROSION FATIGUE FAILURES IN 300M LANDING GEAR STEEL USING MECHANICAL SUPPRESSION

Paul S. Prevéy and N. Jayaraman
Lambda Research
5521, Fair Lane, Cincinnati, OH 45227 – 3401

Neal Ontko, Michael Shepard, Robert Ware and Jack Coate
Air Force Research Laboratory, MLSC, 2179 12th Street, WPAFB, OH 45433

ABSTRACT

300M steel is widely used in landing gear because of its unique combination of ultrahigh strength with high fracture toughness. However, 300M is vulnerable to both corrosion fatigue and stress corrosion cracking (SCC) failures with catastrophic consequences for aircraft landing gear. Plating and shot peening surface treatments currently used to extend life are only partly effective. A surface treatment is needed that will mitigate foreign object damage (FOD), corrosion fatigue and stress corrosion cracking. This paper describes the use of low plasticity burnishing (LPB) to mechanically suppress stress sensitive corrosion failure mechanisms in 3.5% salt solution.

The fatigue and corrosion fatigue performance of LPB processed 300M steel was compared with shot peened (SP) and low stress ground (LSG) conditions. LPB produced residual compression to a depth of 1.27 mm (0.050 in.), and shot peening only 0.127 mm (0.005 in.), an order of magnitude less. LPB treatment dramatically improved both the HCF performance and corrosion fatigue strength, with and without simulated FOD. The corrosion fatigue strengths of LSG and SP surfaces decreased dramatically, to only 20% and 50%, respectively, of the baseline strength, with no discernible endurance limit behavior under corrosion fatigue conditions. The fatigue behavior was even worse with FOD, simulated with a 0.5 mm (0.020 in.) deep EDM notch, both in air and exposed to salt. In contrast, LPB treated specimens with FOD exhibited a definite endurance limit of 1035 MPa (150 ksi) even under corrosion fatigue conditions. SCC testing of LPB treated landing gear sections at 1030 to 2270 MPa (150 to 180 ksi) static loads was terminated after 1500 hrs without failure, compared to failure in as little as 13 hours without treatment.

Mechanistically, the effect of corrosion and FOD resulted in early crack initiation and growth, thus resulting in dramatic decrease in fatigue performance. Despite the existence of similar corrosion conditions, the deep compressive surface residual stresses from LPB treatment mitigated both the individual and synergistic effects of corrosion fatigue and FOD. The deep compressive layer produced by LPB reduced the surface stress well below the SCC threshold for 300M, even under high tensile applied loads, effectively mechanically suppressing the SCC failure mechanism.

Keywords: Residual Stresses, Surface Enhancement, Corrosion Fatigue, Stress Corrosion Cracking (SCC), High Cycle Fatigue (HCF), Low Plasticity Burnishing (LPB), Shot Peening (SP), Foreign Object Damage (FOD)

			Form Approved OMB No. 0704-0188

Report Documentation Page

Form Approved
OMB No. 0704-0188

Public reporting burden for the collection of information is estimated to average 1 hour per response, including the time for reviewing instructions, searching existing data sources, gathering and maintaining the data needed, and completing and reviewing the collection of information. Send comments regarding this burden estimate or any other aspect of this collection of information, including suggestions for reducing this burden, to Washington Headquarters Services, Directorate for Information Operations and Reports, 1215 Jefferson Davis Highway, Suite 1204, Arlington VA 22202-4302. Respondents should be aware that notwithstanding any other provision of law, no person shall be subject to a penalty for failing to comply with a collection of information if it does not display a currently valid OMB control number.

1. REPORT DATE **AUG 2004**	2. REPORT TYPE	3. DATES COVERED **00-00-2004 to 00-00-2004**

4. TITLE AND SUBTITLE **Mitigation of SCC and Corrosion Fatigue Failures in 300M Landing Gear Steel Using Mechanical Suppression**	5a. CONTRACT NUMBER
	5b. GRANT NUMBER
	5c. PROGRAM ELEMENT NUMBER
6. AUTHOR(S)	5d. PROJECT NUMBER
	5e. TASK NUMBER
	5f. WORK UNIT NUMBER
7. PERFORMING ORGANIZATION NAME(S) AND ADDRESS(ES) **Lambda Research,5521 Fair Lane,Cincinnati,OH,45227**	8. PERFORMING ORGANIZATION REPORT NUMBER
9. SPONSORING/MONITORING AGENCY NAME(S) AND ADDRESS(ES)	10. SPONSOR/MONITOR'S ACRONYM(S)
	11. SPONSOR/MONITOR'S REPORT NUMBER(S)

12. DISTRIBUTION/AVAILABILITY STATEMENT
Approved for public release; distribution unlimited

13. SUPPLEMENTARY NOTES
The original document contains color images.

14. ABSTRACT
see report

15. SUBJECT TERMS

16. SECURITY CLASSIFICATION OF:			17. LIMITATION OF ABSTRACT	18. NUMBER OF PAGES **12**	19a. NAME OF RESPONSIBLE PERSON
a. REPORT **unclassified**	b. ABSTRACT **unclassified**	c. THIS PAGE **unclassified**			

INTRODUCTION

SCC, corrosion fatigue, and FOD are generally recognized as significant degradation processes that affect naval aircraft landing gear components. Ultrahigh strength steels such as 4340, AF1410, and 300M are widely used in applications where a combination of high strength and fracture toughness is needed. Most of these ultrahigh strength steels have been known to be prone to SCC and corrosion fatigue.[1-4] The phenomenon of SCC is generally understood to be the result of a combination of susceptible material, corrosive environment, and tensile stress above a threshold, as illustrated in Figure 1. Earlier solutions to reduce the susceptibility to corrosion and the environment have included modifying the material (alloy chemistry), or the use of protective coatings. New alloys[2,3] like Aermet100, Custom250, Custom465, and Allvac240 have shown some improved resistance to SCC. Cadmium and Chromium plating of the steel to retard corrosion and SCC have been standard practice for many landing gear systems[4]. In this paper, a novel approach of "mechanical suppression" of SCC and corrosion fatigue is presented. The method of fully mitigating SCC by keeping the net stresses on the surface to below the threshold value is successfully demonstrated. This is achieved by introducing deep surface residual compressive stresses by LPB.

Introduction of residual compressive stresses in metallic components has long been recognized[5-8] to lead to enhanced fatigue strength. For example, many engineering components have been SP or cold worked with fatigue strength enhancement as the primary objective or as a by-product of a surface hardening treatment like carburizing/nitriding, physical vapor deposition, etc. Over the last decade treatments like LPB[9], laser shock peening (LSP)[10], and ultrasonic peening[11] have

emerged. In all the surface treatment processes, key benefits are obtained when deep compression is achieved with minimal cold work of the surface. All of these surface treatment methods have been shown to benefit fatigue prone engineering components to different degrees.
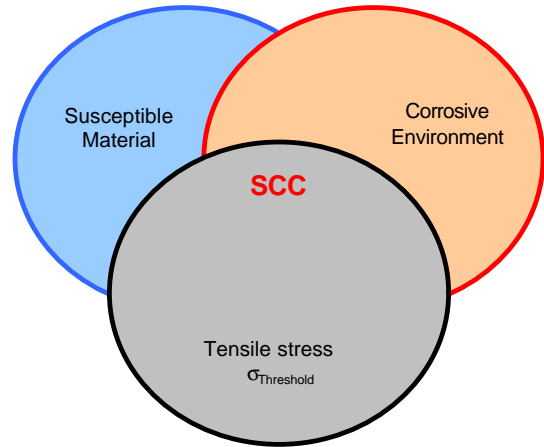

FIGURE 1 - SCC susceptibility diagram illustrating the need for the combination of a susceptible material, corrosive environment and threshold tensile stress to cause SCC.

LPB has been demonstrated to provide a deep surface layer of high magnitude compression in various aluminum, titanium, nickel based alloys and steels. The deep compressive residual stress on the surface of these materials mitigates fatigue damage including FOD,[12-14] fretting fatigue damage,[15-16] and corrosion fatigue damage.[17-20] The LPB process can be performed on conventional CNC machine tools at costs and speeds comparable to conventional machining operations such as surface milling.

The goal of this research was to investigate the effect of a compressive surface residual stress state imparted by the LPB process upon the mechanisms of corrosion fatigue, FOD and SCC in 300M steel. These results are compared with the results obtained after a conventional SP surface treatment.

EXPERIMENTAL PROCEDURE

Material and Heat Treatment

300M steel was procured in the form of 0.5 in. (~12.7 mm) thick plates. Bars of nominal dimensions of 0.375 in. X 1.25 in. X 8 in. (9.5 mm X 31.75 mm X 203.2 mm) were initially machined. All the bars were heat-treated to austenize at 1600ºF (871ºC) and oil quenched, followed by double tempering at 575ºF (302ºC) 8hrs + 8hrs and air cooling to room temperature.

The nominal composition and tensile properties of the heat-treated steel are as follows:

Chemical Composition: (weight%) C-0.41%, Mn-0.76%, P-0.007%, S-0.001%, Si-1.67%, Cr-0.73%, Ni-1.80%, Mo-0.38%, Al-0.040, Sn-0.005, Ti-0.001%, V-0.050, Cu-0.11, Bal-Fe.
0.2% Y.S. = 245 ksi (~1,690 MPa), UTS = 290 ksi (~2,000 MPa), Elong. = 10%, RA = 35%, HRC = 55HCF Specimen Processing

Thick section fatigue specimens were finish machined from the heat-treated bars by LSG. A final heat treatment was performed after LSG. The fatigue specimens have a trapezoidal cross section in the gage region. This design enables the testing of specimens with a deep surface layer of compressive residual stress. The trapezoidal cross section HCF sample was designed to force the fatigue failures to initiate in the compressive gage section surface under 4-point bend loading.

LPB Processing

LPB process parameters were developed by Surface Enhancement Technologies, LLC. (SET) for thick sections of 300M steel using proprietary methods. The CNC control code was modified to allow positioning of the LPB tool in a series of passes along the gage section while controlling the burnishing pressure to develop the desired magnitude of compressive stress with relatively low cold working. Figure 2 shows a thick section fatigue specimen in the process of being LPB processed in the four-axis manipulator on the CNC milling machine.
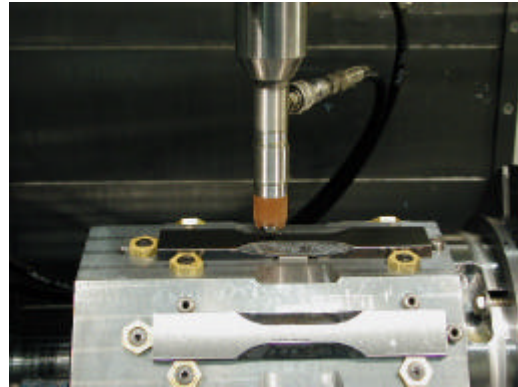

FIGURE 2 - A set of 8 thick section specimens being LPB processed in a 4-axis CNC milling machine.

SP Processing

Shot peening was performed using a conventional air blast peening system equipped with a rotating table on two sets of fatigue specimens with the following process parameters: 150% coverage and CCW14 shot; both 8A and 10A intensities were used for purposes of residual stress measurement, while only SP specimens with 10A intensity were used for fatigue testing. Residual stresses were measured in all surface treated specimens (both LPB processed and SP) before and after exposure to 400°F for 48 hours. The thermal treatment simulates the hydrogen bake-out following cadmium or chromium plating, and allowed examination of any thermal relaxation of residual stresses.

Residual Stress Measurement

X-ray diffraction residual stress measurements were made at the surface and at several depths below the surface on LPB treated fatigue specimens. Measurements were made in the longitudinal direction in the fatigue specimen gage employing a $\sin^2\emptyset$ technique and the diffraction of chromium Ká1 radiation from the (211) planes of steel. The lattice spacing was first verified to be a linear function of $\sin^2\emptyset$ as required for the plane stress linear elastic residual stress model[21-24].

Material was removed electrolytically for subsurface measurement in order to minimize possible alteration of the subsurface residual stress distribution as a result of material removal. The residual stress measurements were corrected for both the penetration of the radiation into the subsurface stress gradient[24] and for stress relaxation caused by layer removal.[25]

The value of the x-ray elastic constants required to calculate the macroscopic residual stress from the strain normal to the (211) planes of steel were determined in accordance with ASTM E1426-9.[26] Systematic errors were monitored per ASTM specification E915.

High Cycle Corrosion Fatigue Testing

All HCF tests were performed under constant amplitude loading on a Sonntag SF-1U fatigue machine. Fatigue testing was conducted at ambient temperature (~72F) in four-point bending mode. The cyclic frequency and load ratio, R ($\sigma_{min}/\sigma_{max}$), were 30 Hz and 0.1 respectively. Tests were conducted to specimen fracture or until a "run-out" life of 2.5×10^6 was attained, whichever occurred first. Run-out specimens were subsequently re-tested to fracture at a minimum stress of at least 20 ksi greater than the stress level at which run-out had first occurred. For analysis purposes, such re-tests were regarded as virgin tests and results were included thus in S-N results. Cycling was terminated upon separation of the sample or when displacement resulting from severe cracking exceeded equipment limits. Specimens from tests terminated for the latter reason were subsequently broken by hand to permit direct observation of fracture surface details.
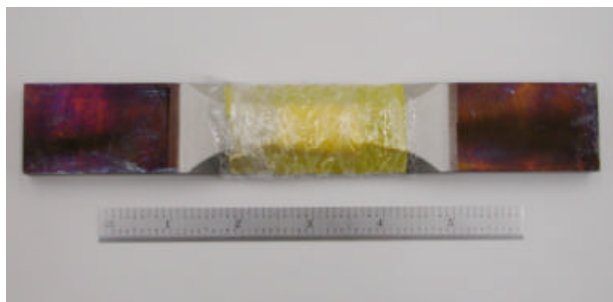
FIGURE 3 - A thick section specimen with salt solution soaked tissue wrapped around the gage section.

Corrosion fatigue testing was performed in a medium of neutral 3.5% NaCl salt solution made using de-ionized water. Filter papers were soaked with the solution, wrapped around the gage section of the fatigue test specimen, and sealed with a plastic film to avoid evaporation. Figure 3 shows a specimen with the acid salt soaked filter paper sealed around the gauge section. To simulate FOD, a semi-elliptical surface notch of depth of a_o=0.020 in. (0.5 mm) and surface length of $2c_o$=0.060 in. (1.5 mm) was introduced in selected groups of specimens by electrical discharge machining (EDM), as shown in Figure 4. Figure 5 shows the specimen mounted in the four-point bend fixture assembled for fatigue testing in a Sonntag SF-1U HCF machine. The following list describes the test conditions used in this study:

	Baseline (LSG)	Shot Peened	LPB Treated
Base (No FOD, No Salt)	✓	✓	✓
Salt Exposure	✓	✓	✓
Simulated FOD	✓	✓	✓
Simulated FOD + Salt Exposure	✓	✓	✓

Due to cumulative corrosion damage, re-testing at higher stresses was not performed on run-out specimens in corrosion fatigue tests.
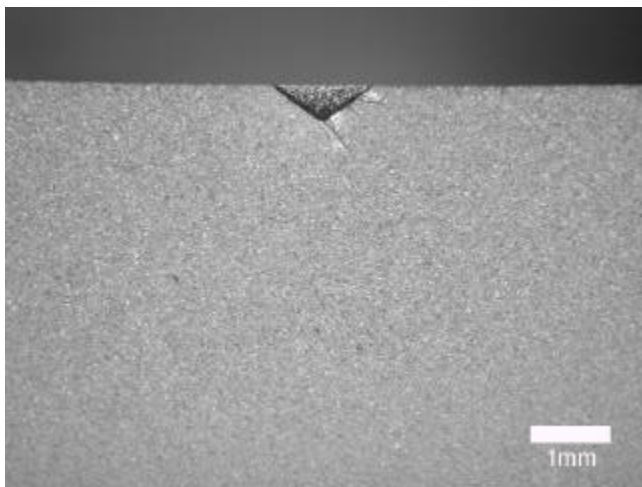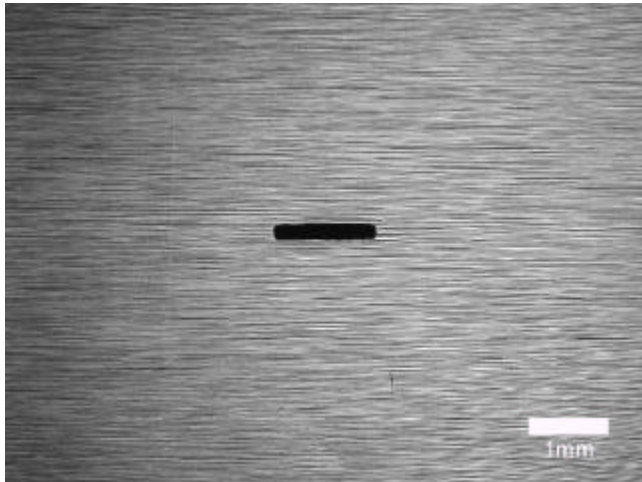
FIGURE 4a.

FIGURE 4 - EDM notch to simulate FOD. (a) Top view, and (b) Cross-section of a 0.020 in. deep notch.
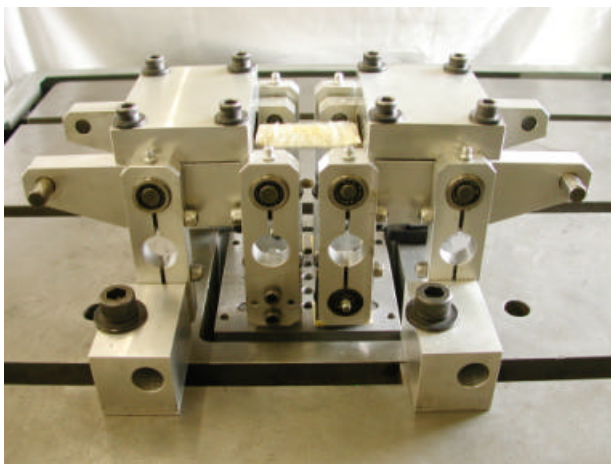

FIGURE 5 - Fatigue test set up.

Stress Corrosion Cracking Tests

SCC tests were performed on C-ring specimens (Figure 6) machined out of an actual landing gear made of 300M steel. The gage region of the C-ring specimen had a cross section similar to the fatigue specimens shown in Figure 2. This design made it possible to investigate the effect of surface treatments like LPB for the SCC tests. Typically, when the specimen is loaded with a bolt through the ¾ in. (19 mm) hole, the outer surface of the trapezoid is in tension, and the tensile stress is uniform over the 1 in. long parallel gage section of this specimen. From the knowledge of the applied forces on the (instrumented) bolt, the bending moment and the corresponding tensile stress on the outer surface can be calculated. Three sets of specimens (both in untreated condition and LPB treated) were SCC tested at 150, 165 and 180 ksi. The SCC test consisted of alternate immersion of the loaded specimen in a neutral 3.5% NaCl solution made with de-ionized water (10 min. in solution and 50 min. in air at room temperature). The load was monitored as a function of time, and the time to failure was noted.
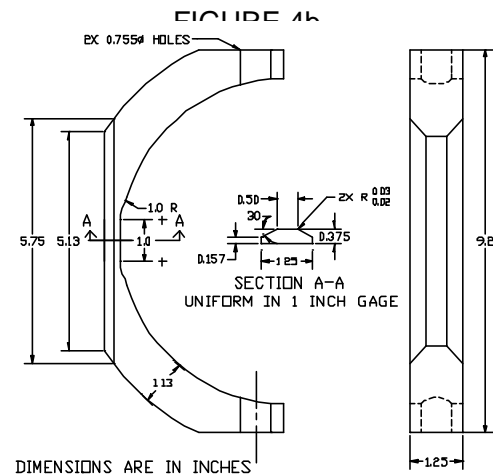

FIGURE 6 - C-ring specimen for SCC tests.

Fractography

Following fatigue testing, each specimen was examined optically at magnifications up to 60x to identify fatigue origins and locations thereof, relative to the specimen geometry. Pictures were taken with a Nikon 990 digital camera through a Nikon Stereoscopic microscope at 15x. A representative photograph of a typical failure for each specimen group was obtained. A few selected specimens were also examined under a Cambridge S90B Scanning Electron Microscope (SEM).

RESULTS AND DISCUSSION

Residual Stress Distributions

The residual stress distributions measured as functions of depth are presented graphically in Figure 7. Compressive stresses are shown as negative values, tensile as positive, in units of ksi (10^3 psi) and MPa (10^6 N/m^2). SP treatment at 8A intensity shows surface compression in the range of −100 to -115 ksi (-690 to -790 MPa), which becomes more compressive to about −150 ksi (-1035 MPa) at a depth of about 0.002 in. (0.05 mm), and rapidly relaxes to nearly zero at a depth of about 0.005 in. (0.125 mm). The 10A intensity of peening introduced a little deeper compression to a depth of 0.007 in. (0.18 mm). The residual stresses from both the SP treatments did not relax significantly after thermal exposure to 400°F for 48 hours. LPB treatment produces surface compression of -100 ksi (-690 MPa), which becomes more compressive to about -180 ksi (-1240 MPa) at depths of 0.005 to 0.020 in. (0.125 to 0.5 mm) and gradually decreases to zero at a depth of about 0.050 in. (1.25 mm). Again, thermal exposure to 400°F for 48 hours did not result in significant relaxation of residual stresses.
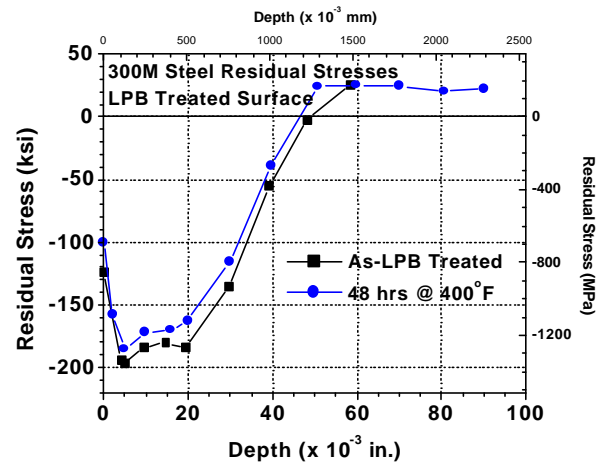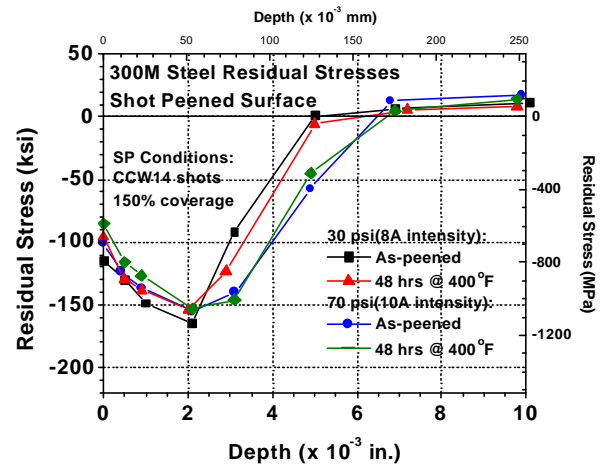

FIGURE 7 - Residual stress distribution for SP and LPB processed specimens. Thermal exposure at 400°F showed no significant effect on residual stresses.

HCF and Corrosion Fatigue Performance

Figures 8-11 show the HCF and corrosion fatigue performance of 300M steel in the form of S-N curves. In Figure 8, the baseline material performance with and without the EDM notch

and exposure to the corrosive environment is presented. The unnotched baseline condition shows a fatigue strength (endurance limit at about 10^7 cycles) S_{max} of about 150 ksi (1035 MPa). In the presence of a neutral (3.5% NaCl) salt solution environment, the corrosion fatigue strength for baseline drops dramatically to about 30 ksi (205 MPa). In fact, the baseline material, which exhibited a strong endurance limit behavior, showed a total loss of endurance strength in the presence of salt solution. Introduction of a semi-elliptical EDM notch of nominal size a_o=0.020 in. (0.5 mm) and c_o=0.030 in. (0.75 mm) drastically decreases the fatigue strength to about 30 ksi (~140 MPa) for air and to less than 10 ksi (70 MPa) for corrosion environment. Power law lines were fitted to the data in Figure 8, and represent the average behavior of the material in its baseline condition.

Figure 9 shows the HCF and corrosion fatigue performance of both unnotched and notched SP treated specimens. Benefits of surface compression from the SP treatment are clearly seen by way of improved HCF performance of the unnotched specimens. Corrosion fatigue strength in the presence of neutral salt environment drops to about 75 ksi (515 MPa). It is interesting to note that this drop of fatigue strength by a factor of 2 is not as severe as the factor of 5 drop seen in the baseline material. The small benefits of shallow compression from shot peening are evident in these results. However, the introduction of a 0.020 in. (0.5 mm) deep notch reduces the performance similar to the notched baseline condition both in air and in the presence of the neutral salt environment. This is not surprising since the corresponding residual stress profile (shown in Figure 7) indicates a depth of compression much shallower than the depth of the EDM notch.
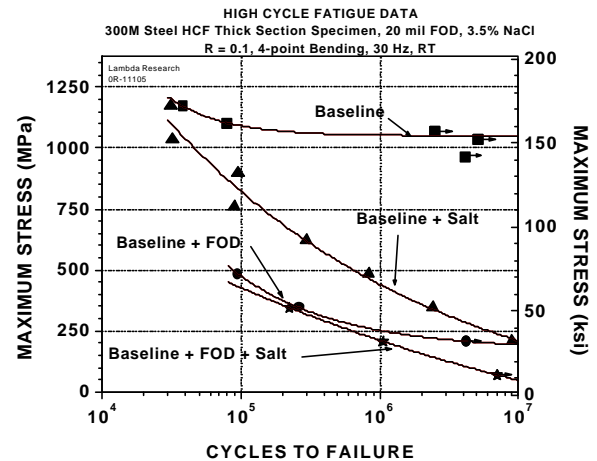

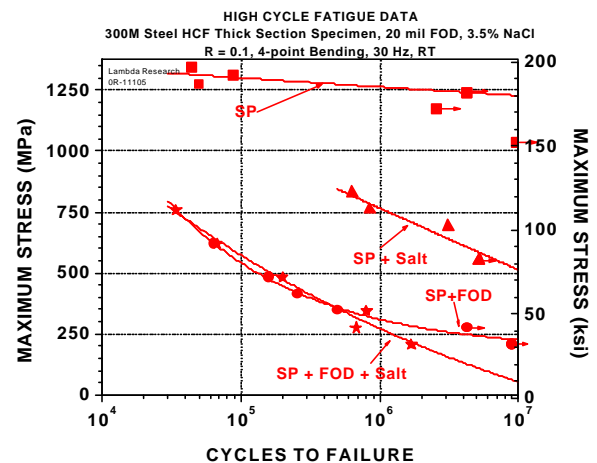FIGURE 8 - Baseline fatigue results
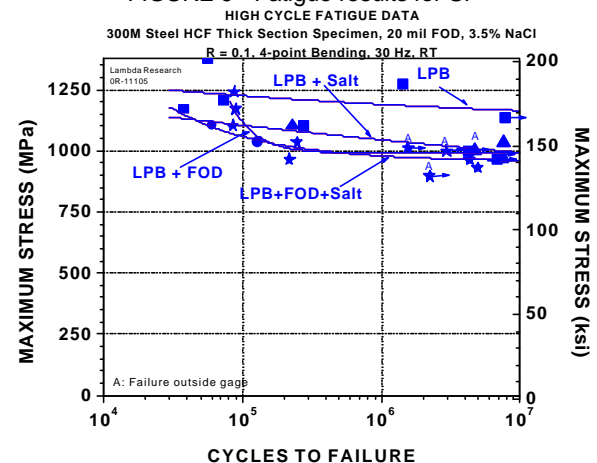

FIGURE 9 - Fatigue results for SP

FIGURE 10 - Fatigue results for LPB
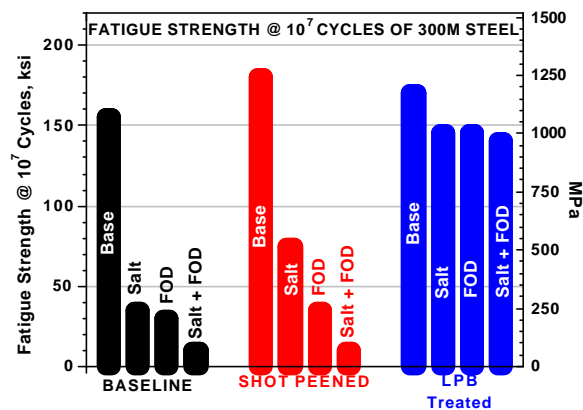
FIGURE 11 - Summary of fatigue results

In Figure 12 the SCC test results show that the untreated baseline material had SCC time to failure of 261.8 hrs at 150 ksi (1034 MPa), 166.5 hrs at 165 ksi (1138 MPa) and 12.9 hrs at 180 ksi (1241 MPa), respectively. The LPB treated specimens did not fail even after 1500 hrs of exposure at all three stress levels. In fact, when the specimens were loaded to higher stress levels in the hope of getting them to crack by SCC, instead of cracking, the specimens were severely bent at higher loads. These results indicate the deep surface compressive stresses from LPB fully mitigated SCC.

Figure 10 shows the HCF and corrosion fatigue behavior of LPB treated specimens. The unnotched specimen shows superior HCF performance with a fatigue strength of 175 ksi (1200 MPa). Figure 10 also shows that fatigue data from all of the other test conditions with LPB treatment. Notched HCF and both notched and unnotched corrosion fatigue test results may be grouped into one set of data at a slightly lower fatigue strength of 145 ksi (1000 MPa). Three conclusions may be reached from this data. First, the LPB process has effectively mitigated corrosion fatigue. Second, the HCF and corrosion fatigue performance of this group is statistically similar to the unnotched baseline material. Third, the endurance limit behavior that was absent in both baseline and SP treatment when tested in the neutral salt solution environment is restored with the LPB treatment.

Figure 11 shows a summary of HCF and corrosion fatigue test results. Here, it is evident that for both baseline and SP materials, a 0.020 in. (0.25 mm) deep EDM notch greatly decreases the HCF and corrosion fatigue strength to a value between 30 and 10 ksi (200 and 70 MPa). In contrast, the LPB treated specimens withstood the same EDM notch with a fatigue strength of 145 ksi (1000 MPa). Again, the HCF and corrosion fatigue performance for the LPB treated specimens are consistent with the residual stress distributions seen in Figure 7.
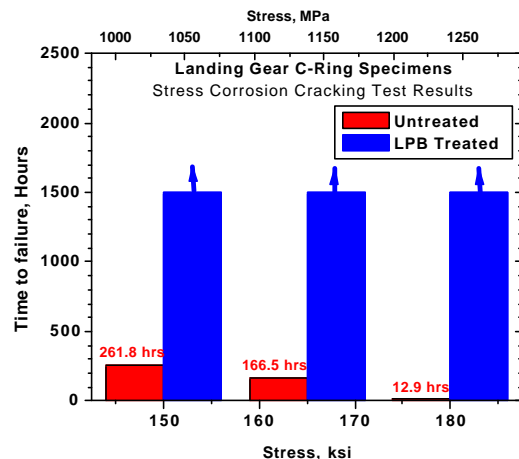

FIGURE 12 - SCC test results.

Fractography

Fractographic analyses presented here are limited to unnotched, corrosion fatigue tested specimens with baseline, SP and LPB conditions. Fractographic analyses of the notched and other HCF test conditions yielded results that are expected and consistent with the fatigue test results shown in Figures 8-11, therefore were not considered to be worthy of inclusion. Figures 13, 14 and 15 show the mechanisms of crack initiation and crack growth under corrosion fatigue conditions, of unnotched specimens. Figure 13a shows the fracture surface of a baseline specimen with a single crack initiation site near the corner of the trapezoidal cross-section. Figures 13b and c show the role of corrosion pits on the crack

initiation process. Similarly Figures 14a, b and c, and Figures 15a, b, c and d show the optical fractographs, the gage of surface with corrosion pits, and the cross-sectional view of a corrosion pit in an unnotched SP and LPB specimen. In all cases, severe pitting of the gage surface is evident, and the cross-sectional views indicate a gradual increase in the depth of corrosion pitting damage with increased time of testing. In both baseline and SP specimens, the corrosion pits resulted in early crack initiation at low stresses, leading to final failure. In contrast, for LPB specimens, despite the higher stress levels and deeper corrosion pitting damage, the corrosion fatigue performance is minimally affected. This is seen in Figures 15a and b, where subsurface crack initiation is evident despite the presence of deep corrosion pits similar to the one seen in the cross-sectional view in Figure 15d.
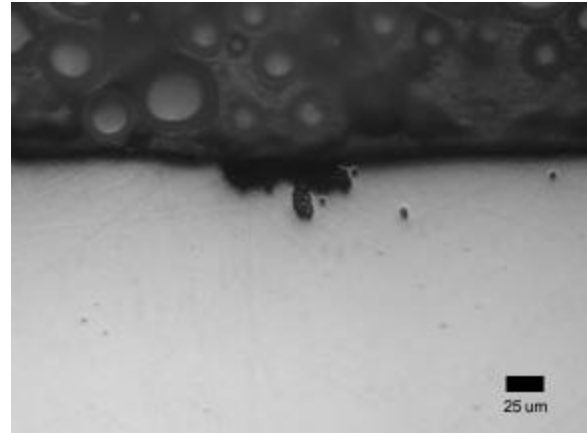
FIGURE 13c

FIGURE 13 - (a) Fracture surface showing crack initiation (arrow) from a corrosion pit, (b) gage surface of the specimen showing a typical set of corrosion pits, and (c) cross-sectional view of a typical corrosion pit in a corrosion fatigue tested baseline specimen; S/N 97, Smax=50 ksi, Nf=2.4(10^6) cycles (~24 hours)
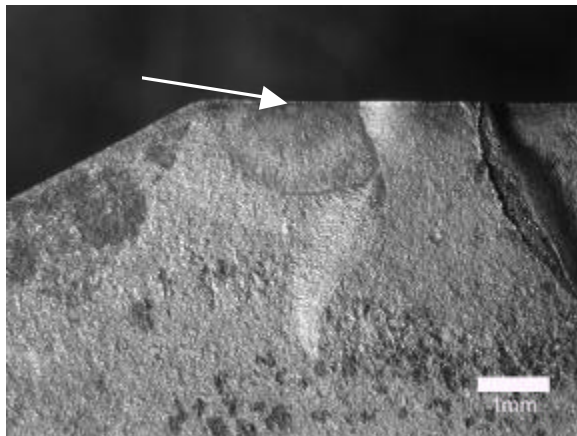

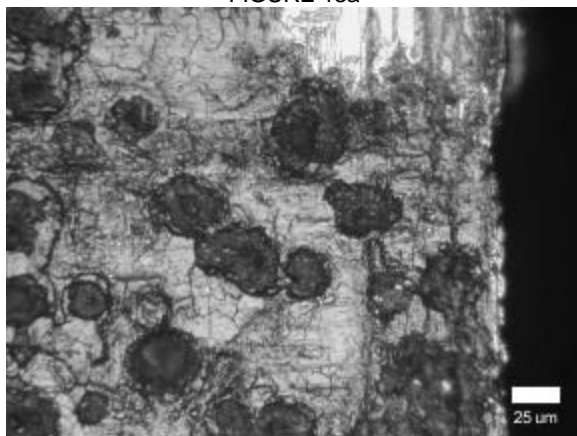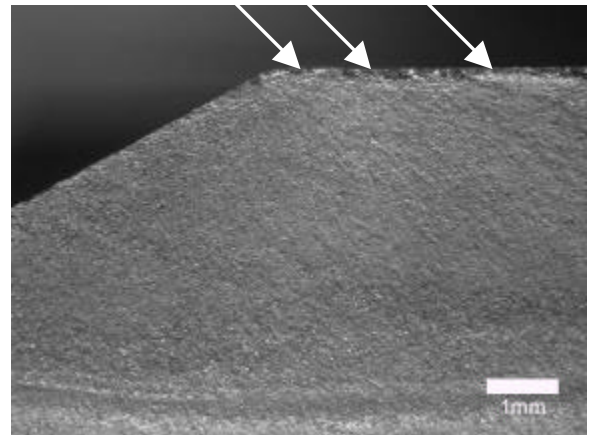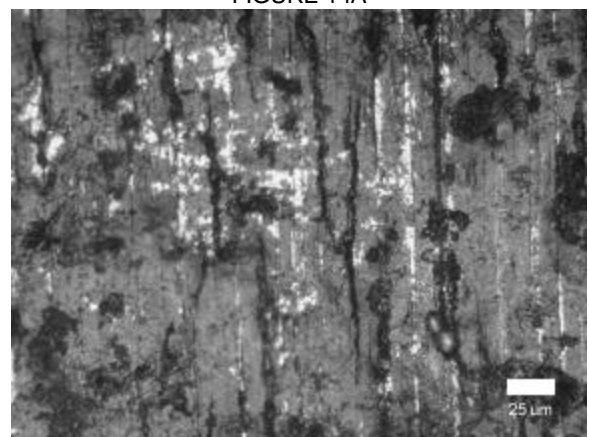FIGURE 13a

FIGURE 14A

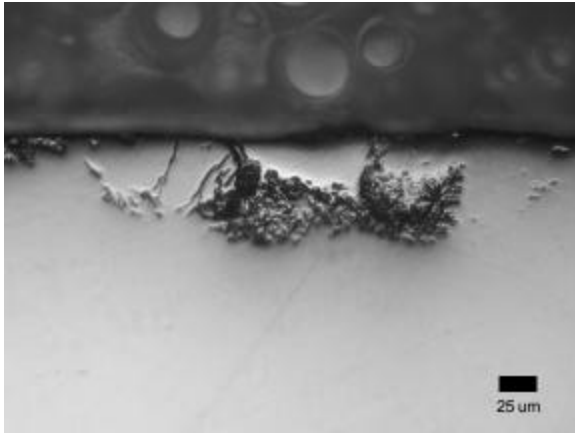FIGURE 13b

FIGURE 14b

FIGURE 14c

FIGURE 15C

FIGURE 14 - (a) Fracture surface showing multiple crack initiation (arrows) sites, (b) gage surface showing a set of typical corrosion pits, and (c) cross-sectional view of a typical corrosion pit in a corrosion fatigue tested SP specimen; S/N 94, Smax=100 ksi, Nf=3.1(10^6) cycles (~30 hours)
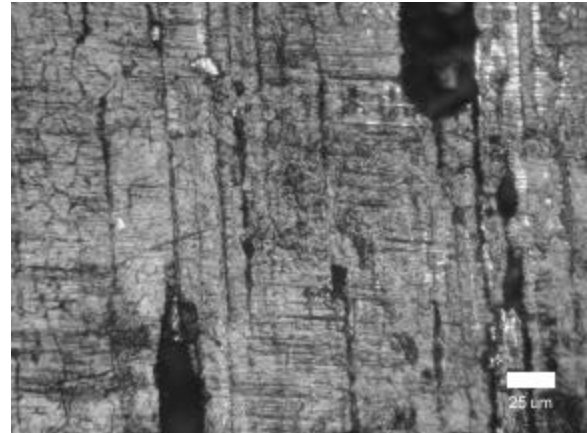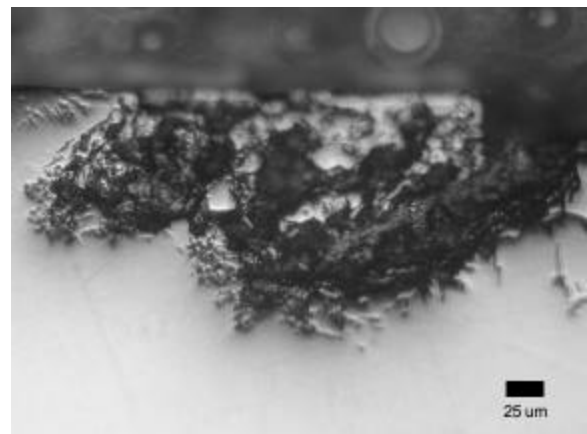

FIGURE 15a

FIGURE 15d

FIGURE 15 - (a) Optical fractograph showing sub surface crack initiation (arrow) site, (b) SEM fractograph showing the same region, (c) gage surface corrosion pits, and (c) cross-sectional view of a typical corrosion pit in a corrosion fatigue tested LPB specimen; S/N 11, Smax=150 ksi, Nf=7.1(10^6) cycles (~70 hours)

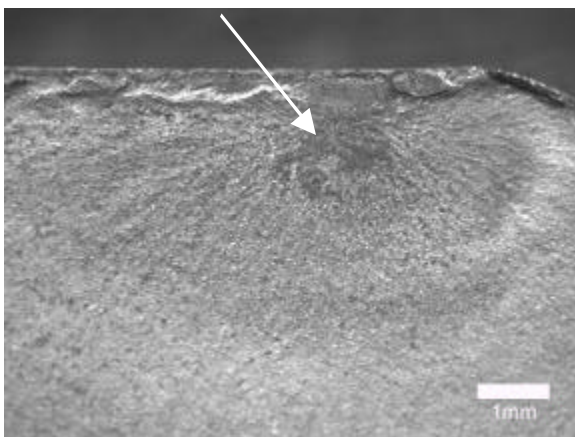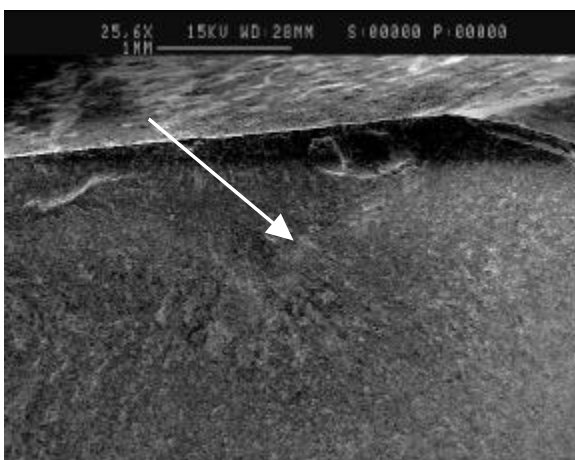FIGURE 15b

SUMMARY AND CONCLUSIONS

In summary, the LPB treatment was studied on 300M steel specimens, which were tested for corrosion fatigue performance and (SCC) in a neutral salt solution environment. The effect of EDM notches to simulate FOD related initial damage conditions were studied. The results overwhelmingly indicate that LPB imparted highly beneficial compressive residual stresses on the surface, and further that LPB treated specimens could easily withstand corrosion fatigue and/or FOD related damage, and successfully resist SCC.

REFERENCES

1. E. U. Lee, C. Lei, H.C. Sanders, R. Taylor, (2004), "Evolution of Fractograph During Fatigue and Stress Corrosion Cracking," Naval Air Warfare Center, Aircraft Div Patuxent River Md, Report Number(S)- NAWCADPAX/TR-2004/12 Unclassified report.

2. E. U. Lee, (1995), Metall. Mater. Trans. A, 26A, (5); May, pp. 1313-1316.

3. Eun U. Lee, "Corrosion Behavior of Landing Gear Steels," Naval Air Warfare Center Aircraft Div Warminster Pa Air Vehicle And Crew Syst Ems Technology Dept, Report Number - NAWCADWAR-94001-60 Unclassified report.

4. "High-Strength Steel Joint Test Protocol for Validation of Alternatives to Low Hydrogen Embrittlement Cadmium For High-Strength Steel Landing Gear and Component Applications", (2003), July 31, Prepared by: The Boeing Company, Phantom Works, Seattle, Washington 98124, and Concurrent Technologies Corporation *(CT*C) Contract #CTC/LAU-CL2402-02 For: Air Force Research Laboratory Task Order 5TS5702D035M.

5. Frost, N.E. Marsh, K.J. Pook, L.P., (1974), *Metal Fatigue*, Oxford University Press.

6. Fuchs, H.O. and Stephens, R.I., (1980), *Metal Fatigue In Engineerin*g, John Wiley & Sons.

7. Berns, H. and Weber, L., (1984), "Influence of Residual Stresses on Crack Growth," Impact Surface Treatment, edited by S.A. Meguid, Elsevier, 33-44.

8. Ferreira, J.A.M., Boorrego, L.F.P., and Costa, J.D.M., (1996), "Effects of Surface Treatments on the Fatigue of Notched Bend Specimens," Fatigue, Fract. Engng. Mater., Struct., Vol. 19 No.1, pp 111-117.

9. Prevéy, P.S. Telesman, J. Gabb, T. and Kantzos, P., (2000), "FOD Resistance and Fatigue Crack Arrest in Low Plasticity Burnished IN718," Proc of the 5th National High Cycle Fatigue Conference, Chandler, AZ. March 7-9.

10. Clauer, A.H., (1996), "Laser Shock Peening for Fatigue Resistance," Surface Performance of Titanium, J.K. Gregory, et al, Editors, TMS Warrendale, PA, pp 217-230.

11. T. Watanabe, K. Hattori, et al,, (2002), "Effect of Ultrasonic Shot Peening on Fatigue Strength of High Strength Steel," Proc. ICSP8, Garmisch-Partenkirchen, Germany, Ed. L. Wagner, pg 305-310.

12. P. Prevéy, N. Jayaraman, R. Ravindranath, (2003), "Effect of Surface Treatments on HCF Performance and FOD Tolerance of a Ti-6Al-4V Vane," Proceedings 8th National Turbine Engine HCF Conference, Monterey, CA, April 14-16.

13. Paul S. Prevéy, Doug Hornbach, Terry Jacobs, and Ravi Ravindranath, (2002), "Improved Damage Tolerance in Titanium Alloy Fan Blades with Low Plasticity Burnishing," Proceedings of the ASM IFHTSE Conference, Columbus, OH, Oct. 7-10.

14. Paul S. Prevéy, et. al., (2001), "The Effect of Low Plasticity Burnishing (LPB) on the HCF Performance and FOD Resistance of Ti-6Al-4V," Proceedings: 6th National Turbine Engine High Cycle Fatigue (HCF) Conference, Jacksonville, FL, March 5-8.

15. M. Shepard, P. Prevéy, N. Jayaraman, (2003), "Effect of Surface Treatments on Fretting Fatigue Performance of Ti-6Al-4V," Proceedings 8th National Turbine Engine HCF Conference, Monterey, CA, April 14-16.

16. Paul S. Prevéy and John T. Cammett, (2002), "Restoring Fatigue Performance of Corrosion Damaged AA7075-T6 and Fretting in 4340 Steel with Low Plasticity Burnishing," Proceedings 6th Joint FAA/DoD/NASA Aging Aircraft Conference, San Francisco, CA, Sept 16-19.

17. N. Jayaraman, Paul S. Prevéy, Murray Mahoney, (2003), "Fatigue Life Improvement of an Aluminum Alloy FSW with Low Plasticity Burnishing," Proceedings 132nd TMS Annual Meeting, San Diego, CA, Mar. 2-6.

18. Paul S. Prevéy and John T. Cammett, (2002), "The Influence of Surface Enhancement by Low Plasticity Burnishing on the Corrosion Fatigue Performance of AA7075-T6," Proceedings 5th International Aircraft Corrosion Workshop, Solomons, Maryland, Aug. 20-23.

19. John T. Cammett and Paul S. Prevéy, (2003), "Fatigue Strength Restoration in Corrosion Pitted 4340 Alloy Steel Via Low Plasticity Burnishing." Retrieved from www.lambda-research.com Sept. 5.

20. Paul S. Prevéy, (2000), "Low Cost Corrosion Damage Mitigation and Improved Fatigue Performance of Low Plasticity Burnished 7075-T6," Proceedings of the 4th International Aircraft Corrosion Workshop, Solomons, MD, Aug. 22-25.

21. Hilley, M.E. ed.,(2003), <u>Residual Stress Measurement by X-Ray Diffraction</u>, HS*J784*, (Warrendale, PA: SAE).

22. Noyan, I.C. and Cohen, J.B., (1987) <u>Residual Stress Measurement by Diffraction and Interpretation</u>, (New York, NY: Springer-Verlag).

23. Cullity, B.D., (1978) <u>Elements of X-ray Diffraction</u>, 2nd ed., (Reading, MA: Addison-Wesley), pp. 447-476.

24. Prevéy, P.S., (1986), "X-Ray Diffraction Residual Stress Techniques," *Metals Handbook*, **10**, (Metals Park, OH: ASM), pp 380-392.

25. Koistinen, D.P. and Marburger, R.E., (1964), <u>Transactions of the ASM</u>, **67**.

26. Moore, M.G. and Evans, W.P., (1958) "Mathematical Correction for Stress in Removed Layers in X-Ray Diffraction Residual Stress Analysis," SAE Transactions, **66**, pp. 340-345.